NUCLEATION AND GROWTH IN THE HYDRIDING REACTION OF URANIUM*

J. B. CONDON

Union Carbide Corporation, Nuclear Division, Oak Ridge, Tenn. 37830 (U.S.A.)

Summary

The growth and nucleation models for uranium hydriding are examined and compared with the experimental behavior of hydriding and dehydriding. Experimental complications such as diffusion limitations, which give rise to several "induction" times, and competing local reactions within a single sample must first be identified and compensated for mathematically before the models for nucleation and growth can be examined. The basis of the models used is the generalized Avrami treatment which utilizes a resultant integral of the rate of formation of growth nuclei and a growth function for each hydride crystallite formed. The following cases are examined using simplified models for the growth function: (1) rapid hydriding where two models could apply; (2) hydriding with the pressure of hydrogen approaching equilibrium, which introduces a new delay time; (3) dehydriding with a rate that must be consistent with the growth function used in hydriding. The usefulness of these models, linked with the diffusion equations, will be illustrated with the calculations of rates of a superficially dissimilar phenomenon, *i.e.* the reaction with water.

1. Introduction

For several years, the U–H system has been investigated at the Oak Ridge Y-12 Plant in order to determine the fundamental properties and parameters that specify the reaction mechanism.

This paper reviews the hydriding and dehydriding mechanism as it is presently understood. An extension of the mechanism to a superficially dissimilar phenomenon, the water oxidation of uranium, is presented. The mechanism quantitatively predicts the reaction behavior under these conditions — notably with the addition of no new parameters.

---

2. Review of the uranium hydriding reaction

The reaction mechanism for hydriding pure unstressed uranium in very pure hydrogen is well known. The overall model is referred to as the per-fusive-precipitation model [1 - 6] (or the perfucipitation model).

The model can be expressed by two simultaneous non-linear differential equations. One is the diffusion equation with a sink and the other is the sink equation

$$\frac{\partial U}{\partial t} = -k_h CU + k_d f(U) \tag{1}$$

where k_h and k_d are the measured hydriding and dehydriding rate constants respectively, C is the mole fraction concentration of hydrogen and U is the normalized medium content. The actual form of $f(U)$ is dependent on the conditions and the sample history.

One of the most interesting boundary conditions to use with the model equations is

$$C(x, t) = C_0 \qquad \text{when } x \leqslant x_s \tag{2}$$

In this condition C_0 represents the solubility of the diffusing species in the material and x_s is the location of a spall front or transformation boundary. For the case of uranium in hydrogen this location x_s is not arbitrary. It is fixed by the fracture mechanics of the material with $x = x_s$ when $U = U_s \approx 0.97$.

From the boundary condition several relationships have been derived [5]. The steady state velocity V_s of the movement of the transformation boundary and the concentration profile C of hydrogen are given by the equations

$$V_s = \frac{-k_h C_0}{\ln U_s} \left(\frac{D}{ak_h U_s}\right)^{1/2} \tag{3}$$

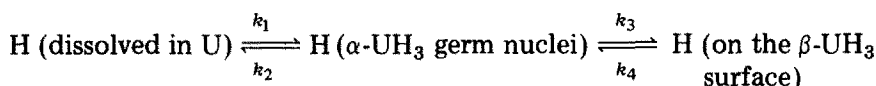$$C = C_0 \exp\left\{-(x - x_s)\left(\frac{ak_h U_s}{D}\right)^{1/2}\right\} \tag{4}$$

The gradient of the product content p is given as

$$\frac{d \ln p}{dx}\bigg|_{x = x_s} = U_s \left(\frac{ak_h U_s}{D}\right)^{1/2} \tag{5}$$

The overall model described so far works well provided that the reacting system is far from equilibrium (but not as far from equilibrium as most oxidations) and that there are few contaminants, especially oxygen, present in the uranium or in the gas phase. The role of oxygen has been described qualitatively [6] in the mathematical model.

3. Derivation and refinement of eqn. (1)

Some pertinent facts about the hydriding system indicate how to derive eqn. (1) in a modified form. In the absence of impurity inclusions the growth of β-UH_3 must occur on spontaneously formed α-UH_3 germ nuclei [7]. Since both α-UH_3 and β-UH_3 are less dense than uranium, compressive stress disfavors the formation of either UH_3. It has been determined, however, that the effect is much greater for β-UH_3 formation than for α-UH_3 formation. For example, Jackson [8] has demonstrated that a sample with greater than 20% cold rolling hydrided slowly at 200 °C in 1 atm pure H_2 to yield at least 50% α-UH_3 on the sample surface. Thus the overall reaction scheme is

$$\text{H (dissolved in U)} \underset{k_2}{\overset{k_1}{\rightleftharpoons}} \text{H (α-UH_3 germ nuclei)} \underset{k_4}{\overset{k_3}{\rightleftharpoons}} \text{H (on the β-UH_3 surface)}$$

The time evolution of the concentration α of germ nuclei can be expressed in terms of itself and the hydrogen concentration by the equation

$$\frac{\partial \alpha}{\partial t} = k_1 C + k_4 - (k_2 + k_3)\alpha \tag{6}$$

The number N of nuclei that become growth nuclei can be expressed in terms of α and a term that expresses the total volume excluded from conversion by stress. This expression is

$$\frac{\partial N}{\partial t} = (k_3\alpha - k_4)\{U - w(\alpha) \int_0^t \dot{N}(\Upsilon)S(t - \Upsilon)\mathrm{d}\Upsilon\} \tag{7}$$

where $S(t)$ is the function expressing the increase in surface area of the crystallite after conversion and $w(\alpha)$ accounts for the depth of this exclusion volume and contains the normalizing units (this also assumes a constant depth regardless of crystallite size, which could be easily changed).

This is similar to Avrami's [9] treatment of phase transformation with modifications in keeping with what is known about this particular system. Avrami's linear grain growth treatment does not explain the second term of eqn. (1) nor does it explain the lack of a large induction time for powder hydriding as the driving force for the reaction is decreased.

Experimental evidence for this latter behavior is shown in Fig. 1. For one case, the initial rate of reaction is about a quarter of the expected rate from the first order expression but no induction time is evident. In neither case is there evidence of deviation toward an exponential dependence on t^2 in place of t as required for the linear grain growth. (Circumstantially, there is also no evidence of needles or dendrites in the product hydride.) This forces the zero or limited growth approximation to Avrami's treatment. This limited growth assumption is consistent with the considerations of the effect of local compressive stress. Following Avrami's treatment the amount of uranium left after time t is
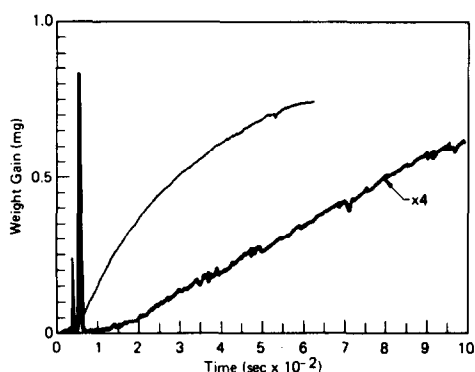
Fig. 1. Weight gain measurement during the dehydriding of a uranium sample. Full stoichiometry is a gain of 3.09 mg. The spike indicates when the hydrogen was admitted. The rapid hydriding was at 172 Pa H_2 and 132 °C to yield a rate of 8.4×10^{-4} s^{-1} compared with 3.2×10^{-3} s^{-1} calculated from eqn. (1). No delay time is observable. The slow hydriding was at 172 Pa H_2 and 180 °C to yield a rate of 5.7×10^{-5} s^{-1} compared with a calculated rate of 2.6×10^{-3} s^{-1}. A delay time of approximately 60 s may be present.

$$U = 1 - \rho \int_0^t \dot{N}(\Upsilon)V(t - \Upsilon)\mathrm{d}\Upsilon \tag{8}$$

where $V(t)$ is a function for volume similar to $S(t)$ and ρ is the conversion factor from volume to normalized U content. The function $V(t)$ is an initially rapidly increasing function the rate of which drops toward zero as local stresses build up.

To obtain the replacement for eqn. (1), eqns. (6) - (8) need to be combined. Even with the exact forms of $w(\alpha)$, $S(t)$ and $V(t)$ known this would be difficult; therefore some simplifying assumptions will be used.

(1) The concentration of α-UH_3 is at steady state, i.e. constant.

(2) The volume function $V(t)$ will be approximated by $V(t) = 0$ when $t < 0$, $V(t) = bt$ when $0 \leqslant t \leqslant t_c$ and $V(t) = V_c$ when $t \geqslant t_c$.

(3) The surface function $S(t)$ is similar to $V(t)$.

The final result is the delay differential–integral equation

$$\frac{\mathrm{d}U}{\mathrm{d}t} = (k_3\alpha_0 - k_4)\left\{ w(\alpha_0)S_c - \frac{V_c + w(\alpha_0)S_c}{t_c} \int_{t-t_c}^t U(\Upsilon)\mathrm{d}\Upsilon \right\} \tag{9}$$

This equation reveals that a phase lag of t_c should be observed if the growth of the crystallites were slow in comparison with the nucleation process. This would be revealed experimentally as an inhibition time on powder hydriding as equilibrium is approached. The data of Fig. 1 indicate that if this is the case then the delay is very small relative to the overall reaction. The term that slows the reaction as equilibrium is approached is $w(\alpha_0)S_c$ and not the phase lag due to slow crystallite growth. Given this information it is reasonable to take the limit of eqn. (9) as t_c approaches zero to

yield eqn. (1) in a modified form:

$$\frac{dU}{dt} = (k_3\alpha_0 - k_4)[w(\alpha_0)S_c - \{\rho V_c + w(\alpha_0)S_c\}U] \tag{10}$$

Not surprisingly this can be made into the form

$$-\frac{dU}{dt} = k_H(C - C_T)\{(1 + R)U - R\} \tag{11}$$

by envisaging a process where equilibrium is "stepped into".

The term $k_d f(U)$ of eqn. (1) no longer appears in this equation in the same form as before. Equation (11) is strictly a microscopic description, and it is believed that the form of $k_d f(U)$ is a consequence of its observation on a macroscopic scale plus the irreversible nature of the integrals used. Equation (4) now becomes

$$C = (C_0 - C_T)\exp\{-(x - x_s)\}\left\{\frac{ak_h(1 - R)U_s}{D}\right\}^{1/2} + C_T \tag{12}$$

Numerical calculations confirm that this steady state condition is approached very rapidly with the hydrogen concentration building up deep inside the solid to a ceiling value of C_T. This fact is very important in application of the mechanism to the water reaction.

4. Application of eqn. (11) to dehydriding

The diffusion equation and eqn. (11) may be solved analytically for a flat plate approximation* [10] if U is assumed to be constant and C is zero at the sample surface. This treatment would probably only be valid for an initial dehydriding (which would be acceptable for the correction term for hydriding) and more detailed knowledge of $V(t)$ as a function of C may be required. For an initial value let $U = R$ from the previous hydriding. R for the dehydriding is assumed to be small ($R(\text{dehydriding}) \approx 0$) since residual compressive stresses should be removed upon dehydriding. From the analytical solution the flux J of hydrogen leaving the particle is given by

$$J = D\frac{\partial C}{\partial t}\Big|_{x=r} = C_T(ak_h UD)^{1/2}\tanh\left\{r\left(\frac{ak_h U}{D}\right)^{1/2}\right\} \tag{13}$$

where the flat plate thickness is $2r$. Since $r \approx 10^{-7}$ m, then the argument of the hyperbolic tangent at 0 °C is about $30\sqrt{U}$. The hyperbolic tangent term then becomes nearly unity for most of the dehydriding. This confirms that the powders under these conditions are "large" pieces [4], for if the argument were sufficiently small the hyperbolic tangent becomes its argument

---

*This approximation has been applied by J. R. Kirkpatrick, Union Carbide Corporation, Nuclear Division, 1979.

and eqn. (13) becomes eqn. (11). Substituting the initial uranium left over from the previous hydriding and converting to proper units, the flux becomes

$$J = 2.4 \times 10^3 R^{1/2} \exp(-8600/T) (\text{g H}) \text{ m}^{-2} \text{ s}^{-1} \tag{14}$$

This expression yields the proper $\Delta H°$ value for the powder dehydriding of 72 kJ (17.2 kcal) compared with the experimental $\Delta H°$ value of 73 ± 3 kJ (17.4 ± 0.8 kcal) [6].

In order to link simultaneous hydriding and dehydriding to calculate rates on very large pieces, a coarse-grained [11] approximation for dehydriding could be linked with the microscopic hydriding to yield a hydride expression such as eqn. (1). This would be sensible if local inhomogeneities in compositions or temperature existed, which is probably true.

5. Calculations for the water reaction

When water reacts with uranium, a great deal of hydrogen is produced. It should be suspected, and has been suggested [12 - 14], that this hydrogen is responsible for the higher oxidation rates observed with water than with pure oxygen.

Experiments utilizing the depth-profiling capability of the ion microprobe mass analyzer (IMMA) were conducted on samples of uranium exposed to sequences of $H_2{}^{16}O$ and $H_2{}^{18}O$. IMMA profiles reveal that the last adsorbed oxygen species is at the metal–oxide interface. A typical result of a two-exposure sequence is shown in Fig. 2 where the exposure was 4 h of $H_2{}^{18}O$ followed by 4 h of $H_2{}^{16}O$ both at 610 Pa pressure and 80 °C. Deuterium labeling combined with oxygen labeling reveals that both hydrogen and oxygen migrate together in some associated form. This form will be referred to here as OH even though the hydrogen and oxygen may only be comigrants. It is believed that this OH migrates interstitially (or possibly by a modified interstitial [15] mechanism) with very little exchange with the UO_2 lattice.

Since the hydrogen migrates with the oxygen to the metal surface, a high hydrogen chemical potential is expected at the interface as the oxygen reacts with the free metal. Oxygen squelches the hydrogen solubility in the metal and, with enough oxygen present or at a low water pressure, the hydrogen profile within the metal will be at the ceiling value C_T regardless of time. If this were the profile under hydriding conditions, nothing would happen. With an excess of oxygen present the overall reaction sequence is shifted to the right. Behind the transformation boundary, $x \leqslant x_s$, the term C_T of eqn. (11) is eliminated. However, since oxygen diffuses slowly in the metal phase, eqn. (11) is undisturbed in front of the transformation boundary. Combining these considerations, the hydriding equation may be used directly with C_T in place of C_0. A comparison of this theoretical minimum rate with the experimental results is given in Fig. 3.
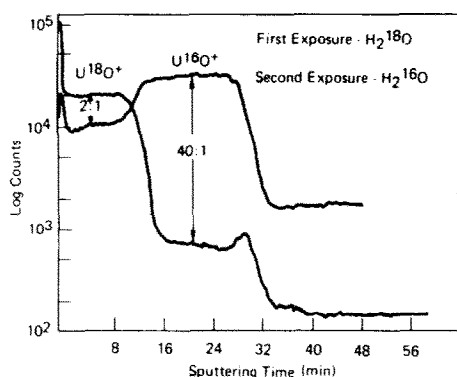
Fig. 2. IMMA depth profile of a uranium sample exposed to 610 Pa $H_2^{18}O$ at 80 °C for 4 h followed by exposure to 610 Pa $H_2^{16}O$ at 80 °C for 4 h. The vacuum–oxide interface is to the left and the metal is to the right.
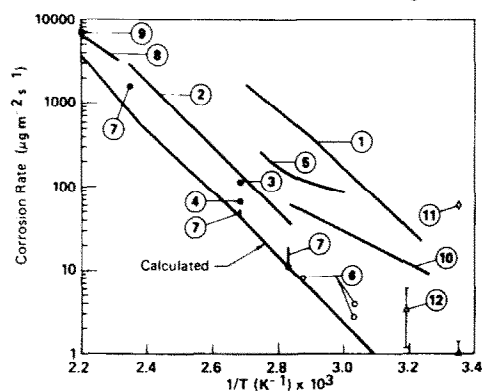

Fig. 3. Comparison of the theoretical minimum rate of reaction of water and uranium with experimental results: 1, liquid H_2O ref. 16; 2, ref. 17 8 kPa H_2O; 3, ref. 17 1 atm O_2, 3.3 - 17 kPa H_2O; 4, ref. 17 as P $H_2O \rightarrow 0$; 5, refs. 13 and 14; 6, ref. 18; 7, ref. 8; 8, ref. 19; 9, ref. 20; 10, ref. 21; 11, ref. 22 electrochemical; 12, ref. 23.
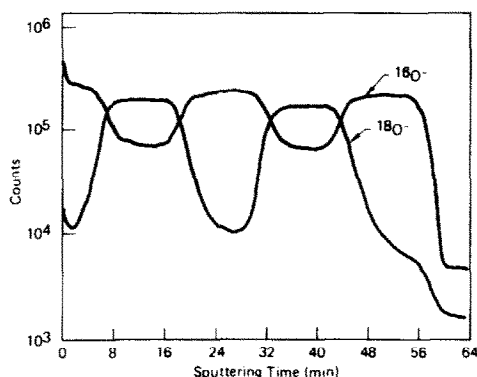
Fig. 4. IMMA depth profile of a uranium sample exposed to the sequence $H_2^{16}O$ for 6 h, $H_2^{18}O$ for 6 h, $H_2^{16}O$ for 6 h, $H_2^{18}O$ for 6 h, $H_2^{16}O$ for 6 h. The pressure for the exposures was 610 Pa and the temperature was 80 °C. The shapes and layer slopes match the model described in the text.

To illustrate the use of eqn. (5) in predicting profile shapes, a sample exposed to the sequence $H_2^{16}O$, $H_2^{18}O$, $H_2^{16}O$, $H_2^{18}O$, $H_2^{16}O$ is shown in Fig. 4. It should be noted that the slopes of the decay of the $^{18}O^-$ profiles are equal for both $U^{18}O_2$ layers. A useful quantity to measure from the IMMA data and to compare with eqn. (5) is the Δx associated with one decade change at the steepest point on the profile. Some corrections must be made for the background base-level and also for the differences in sputtering calibrations and densities for the oxide and metal (13 and 5.3 nm min^{-1} respectively). The calculated values for Δx are the following:

Δx = 15.8 nm calculated from eqn. (5);

$\Delta x \geqslant$ 14.6 nm obtained from the slope of the metal–oxide interface;

$\Delta x \leqslant$ 17.1, 16.3, 16.9 and 15.7 nm obtained from the four slopes representing the isotope switches.

Given the foregoing qualifications, the agreement with the model is quite good in the observed profiles.

6. Conclusions

The hydriding and dehydriding reactions of uranium are probably better understood than most gas–solid reactions. The extension of the mathematical model to calculate both rates and oxide layer structure in the uranium–water reaction without the introduction of any new concepts or parameters is encouraging. There is a high probability that the same mechanism applies to some cases of uranium oxidation with, of course, different parameters for diffusivity etc. It may be that the mechanism can be extended to other metal–gas systems as well.

Acknowledgment

References

1 J. L. Stakebake, *J. Vac. Sci. Technol.*, in the press.
2 J. B. Condon, *J. Phys. Chem., 79* (1975) 392.
3 J. B. Condon, C. E. Holcombe, D. H. Johnson and L. M. Steckel, *Inorg. Chem., 15* (1976) 2173.
4 J. B. Condon, *Y-1963*, October 1974.
5 J. R. Kirkpatrick, *Proc. Hydride Storage Reservoir Symp., June 1978.*
6 J. B. Condon and E. A. Larson, *J. Chem. Phys., 59* (1973) 855.
7 J. B. Condon, *J. Phys. Chem., 79* (1975) 42.
8 R. L. Jackson, personal communication, 1979.
9 M. Avrami, *J. Chem. Phys.,* 7 (1939) 1103; *8* (1940) 212; *9* (1941) 177.
10 H. S. Carslaw and J. C. Jaeger, *Conduction of Heat in Solids*, Oxford University Press: Clarendon Press, Oxford, 1959.
11 J. S. Langer, *Physica (Utrecht), 73* (1974) 61.
12 J. E. Draley and W. E. Ruther, *J. Electrochem. Soc., 104* (1957) 329.
13 T. Kondo, F. H. Beck and M. G. Fontana, *Corrosion (Houston), 30* (1974) 331.
14 T. Kondo, E. D. Verink, F. H. Beck and M. G. Fontana, *Corrosion (Houston), 20* (1964) 314t.
15 C. R. A. Catlow, *Proc. R. Soc. London, Ser. A, 353* (1977) 533.
16 M. McD. Baker, L. N. Less and S. Orman, *Trans. Faraday Soc., 62* (1966) 2513.
17 C. A. Colmenares, submitted for publication.
18 J. T. Weber, *LA-1524*, 1952.
19 B. E. Hopkinson, *J. Electrochem. Soc., 106* (1959) 102.
20 N. Benson, R. P. Straetz and J. E. Draley, *CT-3042*.
21 J. H. Grimes and J. R. Morris, *AWRE 0-68/65*.
22 J. S. Bullock, A. D. Brown and A. G. Dobbins, *Y-1949*, 1974.
23 V. J. Corcoran, C. Johnston, W. J. Metcalfe and J. Thorpe, *AWRE 0-42/65*.